Spring 5-2014

An Approach to Thermocouple Temperature Measurements that Reduces Uncertainties Associated with Radiative Corrections

Siddharth Krishnan
Washington University in St. Louis

WASHINGTON UNIVERSITY IN ST. LOUIS

School of Engineering and Applied Science

Department of Mechanical Engineering and Materials Science

Thesis Examination Committee:

Richard L. Axelbaum, Chair

David A. Peters

Benjamin M. Kumfer

An Approach to Thermocouple Temperature Measurements that Reduces Uncertainties Associated with Radiative Corrections

by

Siddharth Krishnan

A thesis presented to the School of Engineering of Washington University in partial fulfillment of the requirements for the degree of Master of Science

May 2014

Saint Louis, Missouri

Contents

List of Figures

List of Tables

Acknowledgements

I would like to thank Professor Richard Axelbaum for his time, mentorship, support and guidance at every stage of the way. I would like to acknowledge Professor Benjamin Kumfer for many enlightening conversations, and thank Professor David Peters for serving on my committee, and for his help.

Special thanks go out to the members of the Laboratory for Advanced Combustion and Energy Research for their help and support. Thank you also to the departments of Mechanical Engineering and Materials Science, and Energy, Environmental and Chemical Engineering to allow me the opportunity to conduct research in a high-quality laboratory.

Finally, I would like to thank my friends and family for their love and support.

Siddharth Krishnan

Washington University in St. Louis

May 2014

ABSTRACT OF THE THESIS

An Approach to Thermocouple Temperature Measurements that Reduces Uncertainties Associated with Radiative Corrections

Siddharth Krishnan

Master of Science in Mechanical Engineering

Washington University in St. Louis, 2014

Research Advisor: Professor Richard L. Axelbaum

Obtaining accurate temperature measurements in flame environments with thermocouples is extremely challenging due to the effects of radiative heat loss. These losses are difficult to quantify and often cannot be corrected for or minimized without sacrificing spatial resolution. In this work, a new experimental methodology is presented that has shown potential to minimize the temperature correction by both increasing and controlling the effects of convection. This is accomplished through high speed rotation of the thermocouple. The rotation yields a high and known convective velocity over the thermocouple. Heat transfer can then be modeled for the thermocouple, and a functional relationship between temperature and rotational speed can be found. Experiments were conducted over a range of rotational speeds in a control flame with a known temperature to test the feasibility of the rotating thermocouple (RTC) technique for temperature measurements in high temperature gases. The experimental results are shown to closely match the theory for the experimental gas temperature, over a range of rotational speeds, yielding extremely accurate gas temperature measurements. The results also demonstrate minimal perturbation to the flow field, even at high rotational speeds. Additionally, a deconvolution technique is proposed that would significantly enhance the spatial resolution of the technique.

Chapter 1

Background

With efforts to limit global anthropogenic Carbon emissions gaining traction, there is an increased impetus to better understand, control and design large combustion systems. Fig.1.1 is a breakdown of the different sources of energy and the sectors they supply. Between Petroleum, Natural Gas and Coal, it is evident that over 80% of global energy supply comes from fossil-fuel combustion. It bears noting that currently, the combustion of biomass is the dominant contributor (53%) to Renewable Energy.

Figure 2.0 Primary Energy Consumption by Source and Sector, 2011
(Quadrillion Btu)

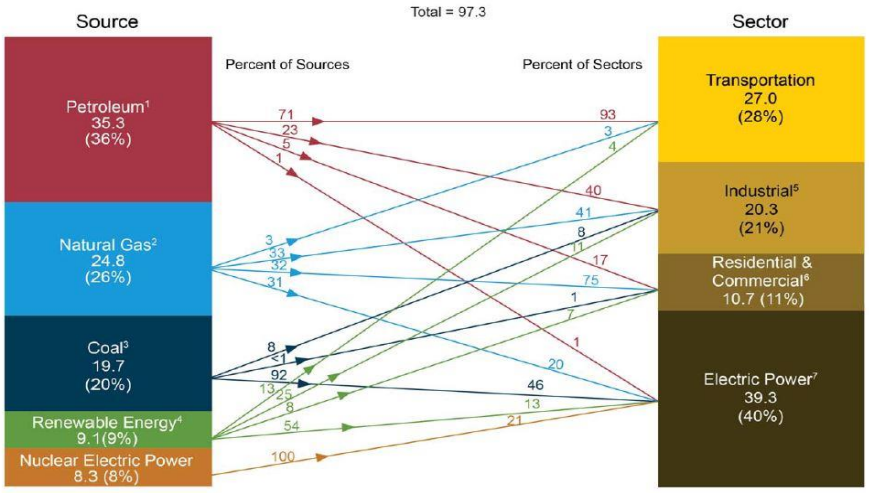

[1] Does not include biofuels that have been blended with petroleum—biofuels are included in "Renewable Energy."
[2] Excludes supplemental gaseous fuels.
[3] Includes less than 0.1 quadrillion Btu of coal coke net imports.
[4] Conventional hydroelectric power, geothermal, solar/photovoltaic, wind, and biomass.
[5] Includes industrial combined-heat-and-power (CHP) and industrial electricity-only plants.
[6] Includes commercial combined-heat-and-power (CHP) and commercial electricity-only plants.
[7] Electricity-only and combined-heat-and-power (CHP) plants whose primary business is to sell electricity, or electricity and heat, to the public. Includes 0.1 quadrillion Btu of electricity net imports not shown under "Source."
Notes: Primary energy in the form that it is first accounted for in a statistical energy balance, before any transformation to secondary or tertiary forms of energy (for example, coal is used to generate electricity). • Sum of components may not equal total due to independent rounding.
Sources: U.S. Energy Information Administration, *Annual Energy Review 2011*, Tables 1.3, 2.1b-2.1f, 10.3, and 10.4.

Fig.1.1. Breakdown of U.S Energy consumption by source [1].

Combined, therefore, combustion accounts for the production of close to 90% of global energy supply. It is evident, therefore, that a better understanding of combustion processes will be integral to the solution of the dual problems of Carbon emissions and meeting the increasing global demand for energy. The accurate measurement of parameters such as temperature and species concentration is integral to such an understanding. The applications of accurate temperature measurement are ubiquitous: the temperature of a flame contains valuable information about the flame's reactions, emissions and the combustors' efficiency, to name just three. Fig. 1.2 is shown the strong relationship between the reaction rate in a reacting flow and the temperature as an illustration of the importance of temperature measurement.

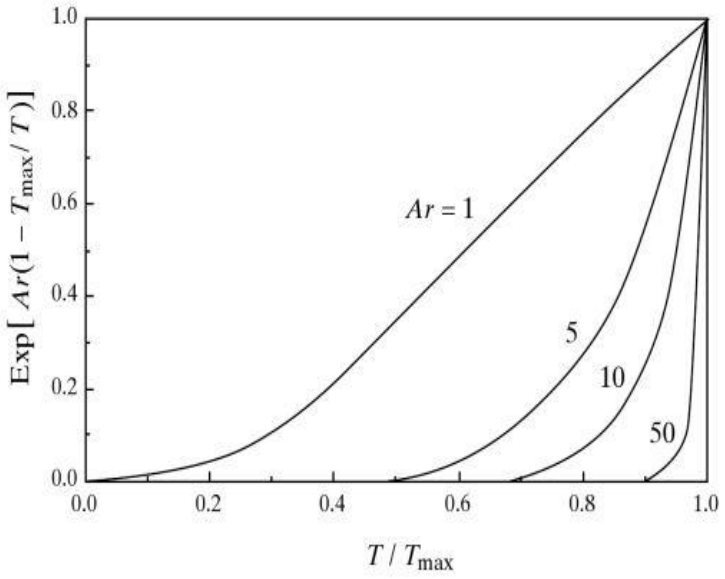

Fig.1.2. Relationship between reaction rate and temperature[2].

These measurements are useful in a wide range of applications, from laboratory–scale flames to combustors and furnaces. A variety of methods have been used to make flame temperature measurements. Broadly speaking, these methods can be classified into optical and probe-based measurements. Though optical approaches to gas temperature measurements provide many

advantages over probe-based methods, they are often difficult to implement, as they can be costly and cumbersome, and are often not effective in particle laden flames or flames involving hydrocarbons larger than methane. Thus, probe-based measurements remain the method of choice for many combustion studies.

Among probe-based measurements, thermocouples have gained preeminence because they are inexpensive, robust and easy to use. The use of fine-wire thermocouples for flame temperature measurements has been extensively discussed [5]. Unfortunately, the use of thermocouples is subject to systematic errors arising from heat losses due to conduction and radiation [4,22-33].

For fine-wire thermocouples, conduction losses are negligible and radiation corrections represent the most difficult challenge to accurate measurement of gas temperatures in flames. Radiation varies with the fourth power of temperature, so a sharp increase in radiation losses from the thermocouple to the environment is observed with increases in gas temperature. At the high temperatures typically encountered in flame environments the temperature error resulting from these losses can be hundreds of degrees [3,4,11]. While often the challenge in laboratory flames is to correct for radiation losses from the thermocouple to the environment, Blevins and Pitt [11] have shown that radiation corrections can also be significant in the cooler parts of a flame where the thermocouple can be radiatively heated by the hot surroundings such as furnace walls or soot particle radiation. Thus, the radiation correction is a complex problem that is difficult to quantify.

Correcting for radiation losses or gains is complicated by uncertainties in variables such as the local convective heat transfer coefficient, the bead size and shape and emissivity and the emissivity of the surroundings. The presence of particles in the flow creates additional

challenges. Many simple algebraic models have been developed to correct for radiation losses [3,11] and some have been validated using CFD models [14]. As radiation gains from the environment are system dependent, no simple models are available for this correction.

One approach to address radiation corrections that has been extensively discussed is the use of multiple thermocouples (typically two) made of identical materials but of different diameters, in order to extrapolate to zero-diameter [6-10]. In unsteady flows the accuracy of this technique is limited by the different time constants of the thermocouples, owing to their different diameters, providing no clear relationship between bead size and temperature. Additionally, there is a dependence on the geometry and orientation of the thermocouples, which makes the technique difficult to implement in many practical combustion systems. However, innovations, like that of Tagawa and Ohta [6], which makes use of advanced digital processing and compensation techniques, continue to be explored.

Perhaps the most widespread approach to addressing the problem of radiation correction is the use of suction pyrometers, otherwise known as aspirated thermocouples, which minimize the effect of radiation losses [11-15,19,36-40]. As the name suggests, suction pyrometers use aspiration to locally extract the combustion gases into a probe. The flow is accelerated within the probe so that it when it passes over the thermocouple the convective heat transfer is high and controlled. Additionally, suction pyrometers are fitted with radiation shields that surround the thermocouple, and an optimum number of shields is used [11]. Suction pyrometers, however, have important limitations. A changing gas sample and long measurement time make it impossible to fit suction pyrometer data to a well-established theoretical curve to yield an

accurate gas temperature. It therefore relies on extremely high aspiration velocities, often on the order of 150 m/s to minimize the value of the error, resulting in extremely poor spatial resolution. Additionally, at typical suction flow rates, on the order of 300 L/min, disturbances to the flow field can be significant. The probes are also large and cumbersome, and can be expensive. Additionally, in particle-laden flows, clogging is a problem, as the molten ash can deposit on surfaces [4]. Finally, the measurement is also affected by geometry and orientation and has a very large time constant [4].

There is a disparity in views with respect to the optimal aspiration velocity. The ASTM recommended value is 5 m/s while others have recommended anywhere between 150 and 200 m/s [11]. This disparity has been discussed by Blevins and Pitts who showed that an aspiration velocity of as low as 5 m/s is usually a significant improvement over an open thermocouple measurement, but operation at this low velocity will result in errors. For example, when the true gas temperature is 927 ºC and the surroundings are at room temperature, the temperature measured by a 1.5 mm thermocouple will increase sharply from 450 ºC to 730 ºC when the aspiration velocity is increased to 5 m/s, and then gradually approach the true gas temperature as the aspiration velocity is increased to 200 m/s,[11], illustrating the diminishing value in operating at higher aspiration velocities.

This study seeks to introduce a new experimental methodology to minimize radiation and conduction corrections, without the level of sacrifice to spatial and temporal resolution that is inherent in aspiration thermocouple measurements. This is achieved by means of a high-speed rotating thermocouple (RTC), which ensures a controlled and high convective heat transfer,

thereby minimizing the effects of radiation and conduction. A detailed description of the methodology and experimental setup follow.

Chapter 2

Theory

Fig. 2.1a shows a thermocouple in a flow of hot gas in an enclosure. A simple heat balance for this thermocouple in steady-state, based on the control volume shown in Fig. 2.1b, is given by

$$\dot{Q}_{conv} + \dot{Q}_{cond} + \dot{Q}_{rad} = 0 \qquad (2.1)$$

It is assumed that thermocouple is convectively heated by the flow of hot gas. It can lose heat by conduction through its wires, and both gain and lose through a radiative exchange with its surroundings. The net radiative heat flux entering or leaving the thermocouple depends on the temperature gradient between the thermocouple and its surroundings, the absorptivity of the thermocouple (here assumed to be equal to the emissivity), ε_b and the emissivity of the enclosure wall ε_w (here assumed to be 1). If the temperature of the enclosure wall, T_w is lower than that of the thermocouple bead T_b , then the net heat radiation heat transfer will be from the bead to the surroundings. In reality, the emissivity of the surroundings and the emissivity of the bead can be difficult, if not impossible, to accurately predict. The emissivity of the surroundings is system-dependent, and in particle-laden flows, it can be particularly difficult to calculate, as it will depend on the volume fraction and the emissivity of the particles, and because the surroundings can change in a reacting flow, thereby resulting in a changing emissivity. The emissivity of the bead can change based on length of exposure to the flow, as it can undergo chemical changes or get coated with soot. The convective heat gain can be expressed simply by Newton's law of

heating/cooling, as being equal to the product of the temperature difference between the gas and the bead, and the convective heat transfer coefficient, given by *h*. The conductive heat loss is directly proportional to the temperature gradient across the wire, given by ΔT, the area of cross section of the wire, A_{cr}, and the thermal conductivity of the thermocouple material, k_b .

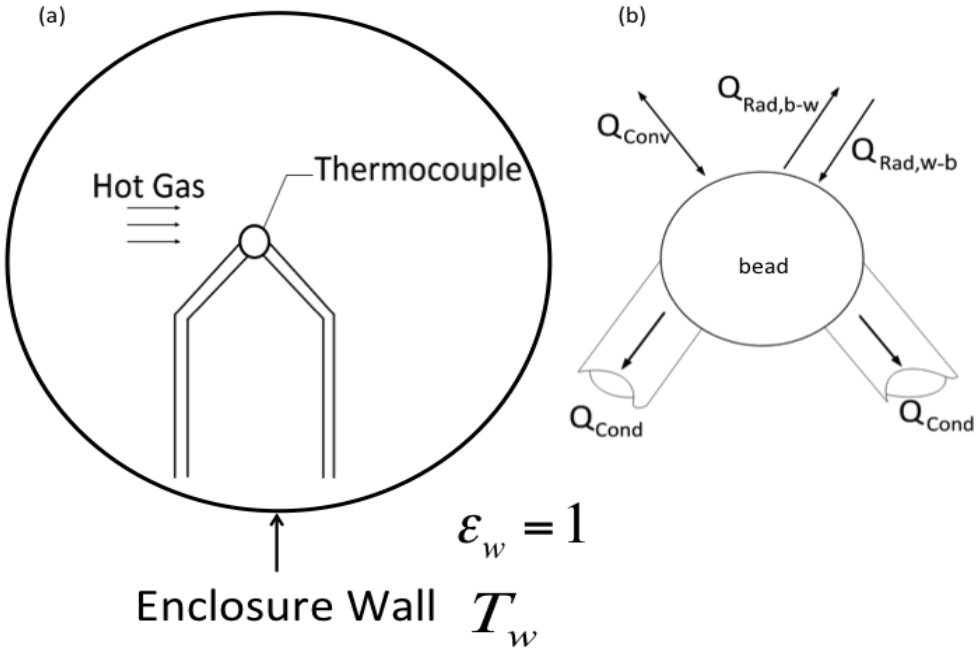

Fig. 2.1. Schematic illustrating heat transfer to and from thermocouple bead. Fig 2.1a shows a thermocouple in a stream of hot gas enclosed in black wall that is at a temperature T_w. Fig 2.1.b shows the control volume of the thermocouple.

Using the above assumptions and simplifications, Eq. (2.1) can be expanded and rewritten as

$$h(T_g - T_b) - \left(\frac{k_b A_{cr}}{L A_{su}}\right)\Delta T - \sigma \varepsilon_b (T_b^4 - T_w^4) = 0 \quad (2.2)$$

Rearranging Eq. (2.2), we get

$$T_g = T_b + \frac{\sigma\varepsilon_b\left(T_b^4 - T_w^4\right) + \left(\frac{k_b A_{cr}}{L A_{su}}\right)\Delta T}{h} \quad (2.3)$$

The second term on the right side of Eq. (2.3) represents a correction, or inaccuracy due to radiative and conductive heat losses.Increasing the value of the convective heat transfer coefficient, *h*, minimizes the value of the correction. The value of *h* can be calculated from the Nusselt number, which is a function of the Reynolds number and the Prandtl number. A generalized form for the Nusselt number is given by

$$Nu_D = CRe^m Pr^n = hD_b/k_g \quad (2.4)$$

The constants *C, m* and *n* vary for different thermocouple geometries, Reynolds numbers and gas compositions. Eq. (2.3) can be rearranged using Eq. (2.4) to yield

$$T_g - T_b = \frac{\sigma\varepsilon_b\left(T_b^4 - T_w^4\right) + \left(\frac{k_b A_{cr}}{L A_{su}}\right)\Delta T}{CRe^m Pr^n\left(\frac{k_g}{D_b}\right)} \quad (2.5)$$

Eq. 2.5 contains a number of terms that are difficult to accurately quantify in industrial-scale, turbulent, particle-laden flames, resulting in large uncertainties in the temperature measurement made by the thermocouple. The Reynolds number is calculated from the local velocity of gas over the thermocouple bead, V_g, which is difficult to measure without altering the flow. Moreover, in a turbulent system, V_g can change on extremely short time-scales, further compounding the problem. The uncertainties in the emissivities of both the surroundings and the bead have already been discussed. The gas-properties, such as the Prandtl number and k_g have a strong temperature dependence, and cannot be accurately predicted without knowing T_g. Finally, there are uncertainties inherent to thermocouples, such as variations in the

thermocouple composition or size could also be present. This final class of uncertainties is usually small. However, if the thermocouple is rotating, a number of positive developments occur.

First, the linear speed of the bead, V_b, is a function of the rotational speed, ω, and if the rotational speed is fast enough that the surrounding gas velocity is small compared to V_b, then V_{tot}, the total relative velocity between the bead and the gas can be approximated by

$$V_b \approx \frac{2\pi r\omega}{60} \qquad (2.6)$$

where *r*, the radius of the circular motion of the thermocouple. Here *r* becomes a design parameter that dictates how rotational speed, in revolutions per minute (rpm) translates into linear speed, in meters/second (m/s). This demonstrates one of the important benefits of the spinning thermocouple: while the gas velocity over a thermocouple is typically unknown, spinning the thermocouple at sufficiently high speed removes this uncertainly since the gas velocity over the thermocouple is now defined by the known rotational speed of the thermocouple.

Combining Eqs. (2.5) and (2.6), we obtain

$$T_g - T_b \approx \frac{\sigma\varepsilon_b\left(T_b^4 - T_w^4\right) + \left(\frac{k_b A_{cr}}{LA_{su}}\right)\Delta T}{C\left(\frac{\rho 2\pi r\omega D_b}{\mu 60}\right)^m Pr^n\left(\frac{k_g}{D}\right)} \qquad (2.7)$$

Eq. (2.7) provides us with a functional relationship between the rotational speed, the diameter of the thermocouple and the correction. This reveals another advantage of spinning the thermocouple: as the denominator assumes high values, i.e., ω is increased, the magnitude of the correction decreases.

To gain an appreciation for the magnitude of the effect of spinning for realistic values of rotational speed and bead size, the following assumptions are made. A flame temperature of 1700 K is used and *r* is assumed to be 12 mm. The gas properties are evaluated at 1700 K and are obtained for nitrogen since a large amount of the combustion product gas will be nitrogen. The kinematic viscosity, ν, is taken to be $27.5 \times 10^{-5} m^2/s$, the thermal conductivity, *k*, to be 0.09W/ m-K, and the Prandtl number to be 0.73. The temperature of the surroundings, T_s, is taken to be 300 K. For the thermocouple bead an emissivity value of 0.1 for uncoated platinum is assumed and conduction losses are neglected.

Using the assumptions listed above, the Reynolds number is shown in Fig. 2a for a range of rotational speeds as a function of the thermocouple bead diameter. In Fig. 2b this is translated into *Nu* for a bead diameter of 0.203 mm., As thermocouple beads are sometimes better represented by a sphere or a cylinder,, which have different values for *C* and *m* in Eq. (2.4), both geometries are considered in Fig. 2.2b.

In Fig. 2.3, the normalized bead temperature, *T**, as obtained from Eqn. (2.7), is plotted, using the Churchill-Bernstein correlation for the Nusselt number for flow over a cylinder. The

normalized temperature is the ratio of the thermocouple bead temperature T_b, to the true gas temperature T_g, in degrees Kelvin, and is plotted as a function of rotational speed for various bead diameters. The smaller thermocouple bead size results in smaller radiative losses because of the reduced surface area. A key observation from this figure is that the effect of rotational speed on temperature T^* is significant, and T^* asymptotes to unity for realistic rotational speeds. The effect of spinning is much more significant at low rpm.

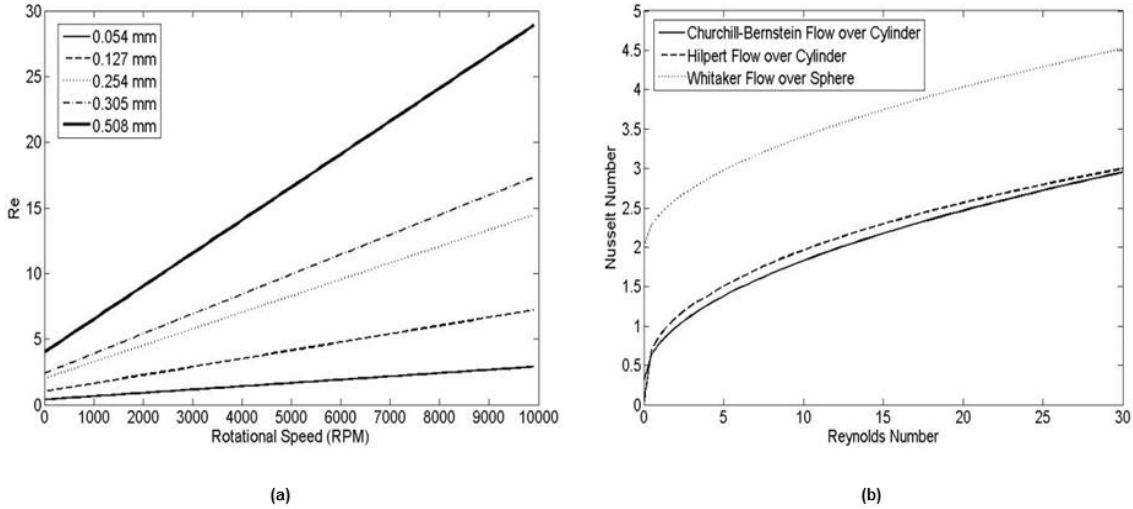

Fig. 2.2a The Reynolds number plotted as a function of rotational speed for different bead diameters. The sizes of the wire diameters used correspond to the diameters of a standard fine-wire thermocouple wires;. b. The Nusselt number plotted for cylindrical and spherical bead geometries for a range of Reynolds numbers corresponding to rotational speeds of interest.

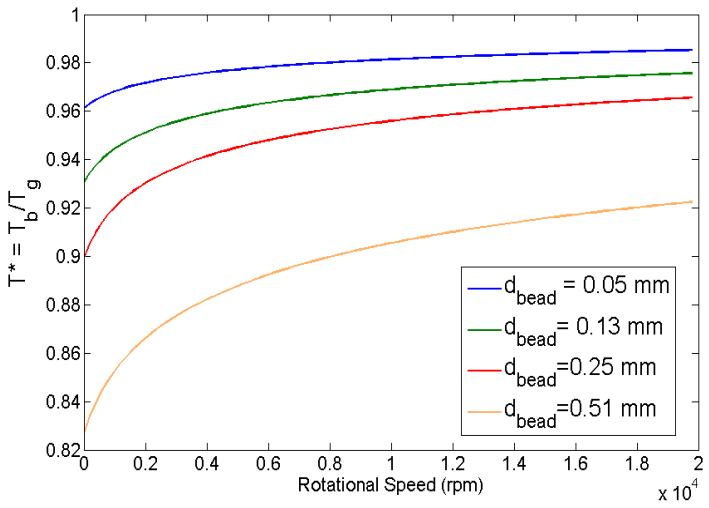

Fig. 2.3: The normalized temperature, which is the ratio of the thermocouple bead temperature, T_b to the true gas temperature T_g plotted as a function of rotational speed. The effect of rotational speed on temperature shows T* asymptoting to 1 as the rotational speed increases to infinity.

Based on this information an experimental apparatus was constructed to test the feasibility of this concept for measuring gas temperature in hot environments.

Chapter 3

Experimental Design

A schematic of the system is shown in Fig. 3.1. A hollow shaft made of 347 grade stainless-steel with a 12.7 mm outer diameter, 3.18 mm inner diameter, and 165 mm length is fitted with an uncoated platinum-platinum/rhodium 10% (Type S) thermocouple. The diameter of the thermocouple wire is 0.13 mm, and the size of the bead in these experiments is 0.20 mm. The wire diameter chosen represents an optimum, as it is significantly more robust than finer wire thermocouples while also being thin enough to minimize conduction losses. Experiments were also conducted with a 0.05 mm diameter thermocouple, and stroboscopic measurements revealed that the thermocouple maintained its shape and did not deform while being spun. Nonetheless, the robustness of such a small thermocouple wire in turbulent, particle-laden environments is questionable. Thus, experiments were conducted with the larger wire size of 0.13 mm diameter. The main drawback of the larger wire size is the larger heat loss corrections due to radiation and conduction, which this work seeks to address.

The thermocouple wire is housed inside a 99% alumina ceramic sheathing and the wires protrude 14 mm from holes in the ceramic sheathing, and are bent at nearly right angles to the longitudinal axis of the shaft, thereby creating a radius of 14 mm. The shape of the thermocouple bead that was used more closely resembles a cylinder than a sphere, though it is not perfectly cylindrical.

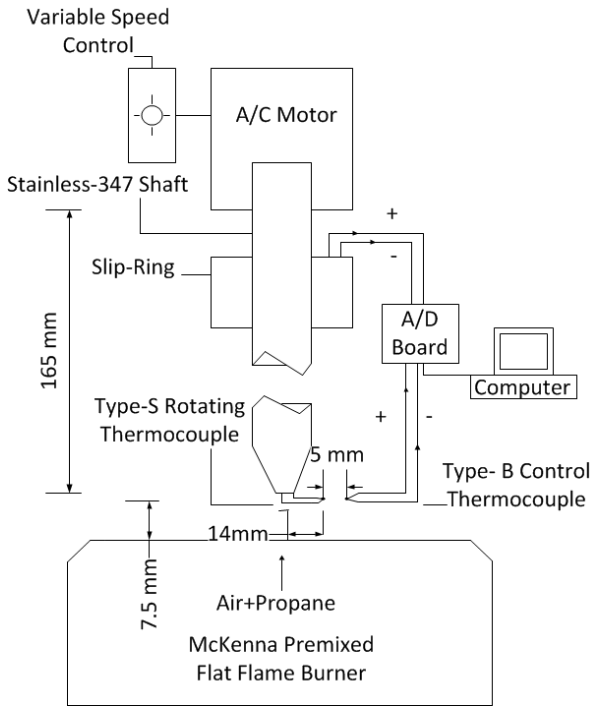

Fig. 3.1. Schematic of Experimental setup.

The shaft is mounted to an AC motor that is equipped with a variable speed control and the rotational speed can be varied from 0 to 23,000 rpm. The rotational speed is measured using a non-contact laser tachometer. The low-voltage thermocouple signal is transmitted by means of a slip ring-brush system (Fabricast Inc., South El Monte, California) that is specifically designed for thermocouple measurements. The analog signal is converted into a digital temperature reading using an MC USB-TC (Measurement Computing, Norton, MA) A/D board. The signal is converted to a temperature using a Type S calibration curve and fed to a computer where it is recorded in real-time using LabView (National Instruments, Austin, TX) software.

For this feasibility study, the goal was to validate the functional dependence between T_b and ω thereby yielding an accurate value for T_g. In order to validate this value for T_g predicted by the RTC, it was compared with a value for T_g that was calculated from a radiation correction. A flat-flame was chosen as the experimental flame because of its controlled, known local velocity (calculated from calibrated rotameters), minimal temporal variation with temperature and well-characterized temperature distribution [19,20]. The assembly was mounted over a McKenna premixed flat-flame burner, The 60 mm-diameter burner head is composed of sintered stainless steel that is water-cooled. The burner was fed with a propane-air mixture, and was shielded with an inert nitrogen shroud. The bead of the thermocouple was 7.5 mm above the visible part of the flame, and no disturbance to the flame was perceptible under these conditions. The sampling rate for these experiments was arbitrarily chosen to be 2 Hz, as the flame was in steady state and displayed negligible temporal variation in temperature. Three flames were produced for the experiments, with equivalence ratios of φ=1, 0.85 and 0.70, respectively, each of which produced a flame of a different temperature. Catalytic effects, while often significant, can be neglected here because the thermocouple is in the post-flame region and the premixed system operates with a fuel-lean stoichiometry The existence of temperature gradients across the McKenna burners has been previously studied [18], and for these experiments, a zone displaying minimal temperature variations was identified and used. Over the 44 mm circumference traced out by the spinning thermocouple, a temperature variation of 35±5 K was observed for all three flames. To obtain the average temperature over this circumference, temperature measurements were taken at 44 points around the circumference, with each measurement roughly 1-mm apart, and the average of these measurements was computed. A radiation correction was performed

on this average temperature to yield a value of the average gas temperature T_g with relatively low uncertainty.

Additionally, a control thermocouple was constructed of Pt 30% Rh-Pt 6%Rh (Type B) alloy, with 0.20 mm bead diameter. This "control thermocouple" was placed in the flame at the same height as the rotating thermocouple ± 1 mm, but at a distance of 5 mm from the rotating thermocouple at its closest location during rotation. This second thermocouple was used to evaluate the effect of flame perturbation caused by the high-speed rotation, and the data was recorded simultaneously with the RTC as part of the same experiment, also at a sampling rate of 2Hz.

The stainless steel supporting rod and motor, shown in Fig. 4, were not cooled in this experiment because the heat from the flame products could be easily shielded from the rod and other components, so that the temperatures were never too high. In practice, for example in a furnace, these parts would need to be cooled to ensure that the temperatures of these components are never too high. In particular the stainless rod, which must protrude into the flame, would need to be shielded, *e.g.*, with a water jacket, to keep it from warping.

The slip-ring bearings exhibited frictional heating. This heating led to a well-defined error in the signal, which was on the order of 7 K at 10,000 rpm, and virtually nonexistent below 5,000 rpm. The error was corrected for using a calibration.

Chapter 4

Results

The RTC assembly was mounted such that the plane of rotation for the thermocouple was parallel to the surface of the flat-flame burner. Fig. 4.1 shows raw data to allow the dynamics of the system to be observed.

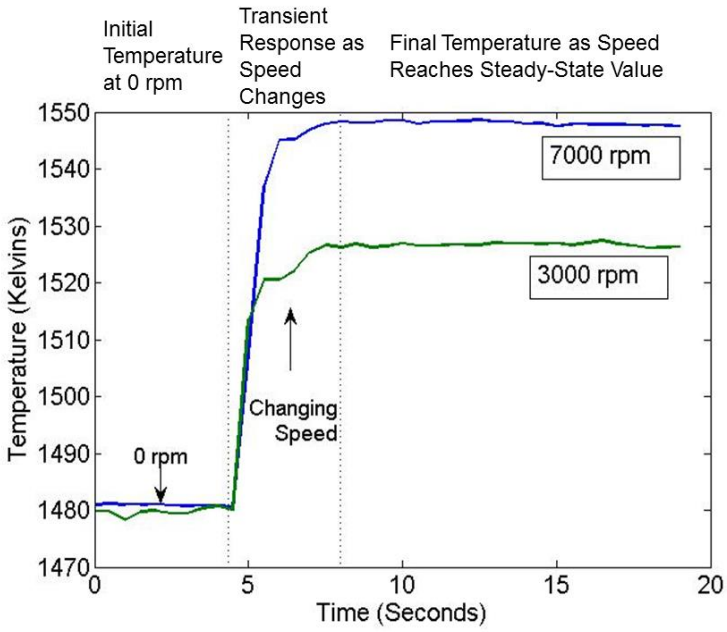

Fig. 4.1. Dynamics of RTC: Experimental data showing transient temperature measured by RTC during the changing of rotational speed, demarcated into transient zone and steady-state zones for two different rotational speeds, 3000 and 7000.

Once the flame was lit, the thermocouple was kept stationary until it reached its steady-state temperature of 1480 ± 2 K. The motor was then ramped up to a steady-state rotational speed of 3,000 rpm. Of course, this was not an instantaneous change and the ramping time was on the order of 2 seconds. The temperature was then allowed to reach its steady-state value of 1525 ± 2 K at a rotational speed of 3,000 rpm. The experiment was repeated, and this time the motor's speed was ramped up to 7,000 rpm, and once again was allowed to reach its steady-state temperature of 1550 ± 5 K. As expected, the temperature registered by the rotating thermocouple, T_b, is strongly dependent on rotational speed. Images were recorded of the RTC in motion at each of the rotational speeds discussed and are shown in Figs. 4.2. a-d. Fig. 4.2a shows the system with more light to clearly illustrate the flat-flame and the relative position of the RTC. Figs. 4.2b-d are shown with reduced aperture to clearly show differences in the brightness of the RTC. The increased brightness of the RTC at 7,000 rpm over that at 3,000 rpm is clearly visible, and is consistent with the data shown in Fig. 4.1.

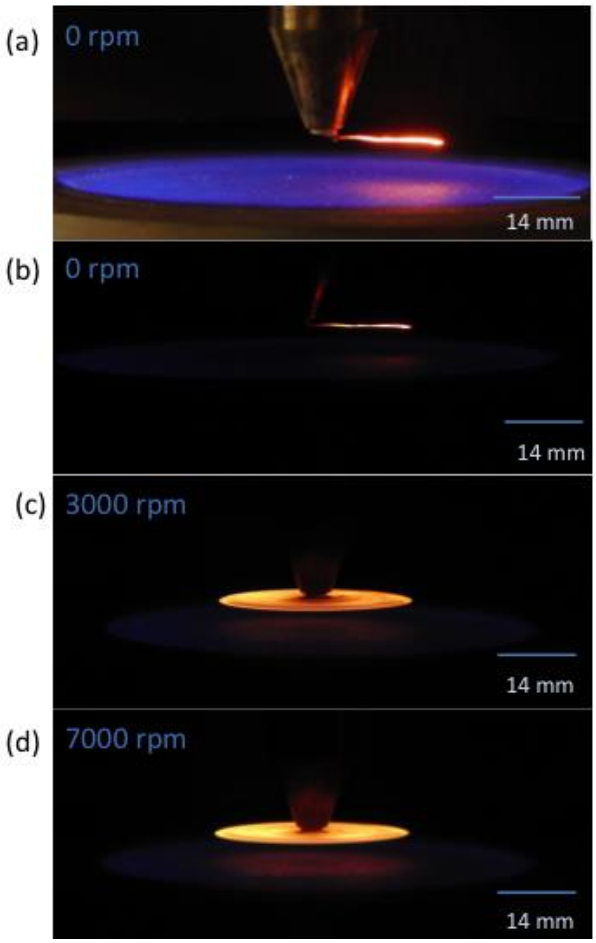

Fig. 4.2. Images of (a) RTC stationary in McKenna flat-flame burner at (b) 0 rpm, (c) 3000 rpm and (d) 7000 rpm.

In the next series of experiments, three separate flames were produced, each with a different equivalence ratio. The thermocouple was rotated at a range of rotational speeds between 0 and 10,000 rpm and allowed to come to steady-state at each speed and data was then recorded for 10 seconds and averaged, and shown in Fig. 4.3. The variation in temperature at each speed was

minimal, on the order of 1 K. The true gas temperature T_g was calculated using a semiempirical curve-fit of the data, and is shown in each figure.

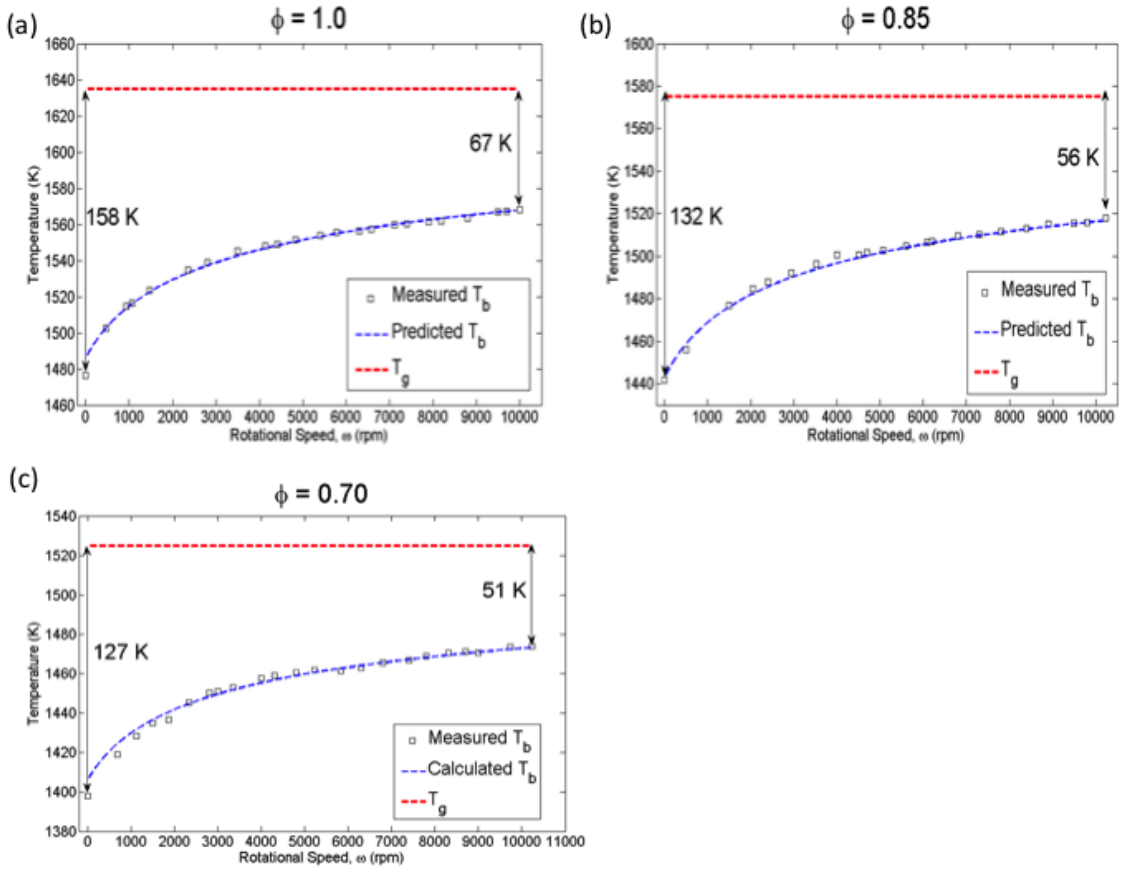

Fig. 4.3. Relationship between temperature and rotating speed for RTC: Experimental temperatures measured by RTC plotted against rotational speed for a) φ=1.0, b) φ= 0.85 and c) φ = 0.70. The true gas temperature is presented with the horizontal dotted line, and the simulated curve predicted by the theory is included for each flame.

In this case, since the velocity and composition of the gas are known, the radiation correction on the stationary reference thermocouple is reasonably accurate. Visual inspection of the

thermocouple bead suggested that its shape closely modeled a cylinder, so the Churchill-Bernstein correlation for flow over a cylinder was used to calculate the theoretical Nusselt number at each rotational speed and gas properties such as the Prandtl number, kinematic viscosity and thermal conductivity were evaluated assuming air at a film temperature of 1200ºC. Using these assumptions, a theoretical curve was fit to the RTC data and the gas temperature that yielded the best fit with the data was obtained. Conduction losses are negligible here because of the high aspect-ratio of the thermocouple wire. The gas temperature predicted by RTC is in excellent agreement with the radiation-corrected value of the gas temperature. These results are summarized in Table 4.1.

Table 4.2: Difference between radiation-corrected gas temperatures and curve-fit predicted temperature from RTC

Φ	T_g calculated from Radiation Correction Performed on Bare-Bead Thermocouple (Degrees Kelvin)	T_g Predicted by Semiempirical curve-fit of RTC data (Degrees Kelvin)
1.0	1621	1635
0.85	1574	1575
0.70	1510	1525

Chapter 5

Discussion

5.1 Relationship between Temperature and Rotational Speed

It can be seen from Figs. 4.1, 4.2 and 4.3 that an increase in rotational speed causes an increase in measured temperature that is extremely smooth, and importantly, is in excellent agreement with the expected shape from theory. The lack of mechanical deformation of the 0.127 mm wire when being spun is an important result, as it displays the feasibility of using a relatively thin wire in the RTC, and the high aspect-ratio of such a wire means that conduction losses can be neglected.

A minimal number of assumptions were made in arriving at the simulated curves shown in Fig. 7. The semiempirical results are in excellent agreement with the data, indicating that the theory accurately captures the heat transfer occurring to and from the thermocouple for the complete range of rotational speeds studied in this work. The predicted gas temperatures for the three cases studied are within 14 K, 1 K and 15 K of the true gas temperatures, as seen in Table 4.1. This result yields accuracy that has been previously unattainable in gas-temperature measurements without significantly sacrificing spatial resolution. Moreover, this accuracy is virtually impossible to attain with a suction pyrometer, because of the changing gas sample and is further complicated by the long measurement time of the suction pyrometer.

In the three flames studied, the RTC measured temperatures when rotating at 10,000 rpm were within 54 K, 66 K and 36 K of the true gas temperature, which is a significant reduction in the correction needed over that of a stationary thermocouple. These results are summarized in Table 5.1.

Table 5.1: Summary of reduction in correction achieved by high-speed rotation.

	Magnitude of Correction (Kelvins)	
Φ	**Stationary Thermocouple (Degrees Kelvin)**	**RTC (Degrees Kelvin)**
1.0	158	67
0.85	132	56
0.70	127	51

The results suggest that by high-speed rotation, the magnitude of the required correction can be significantly reduced.

5.2 Spatial Resolution

The improvement in spatial resolution of measurements made by the RTC over suction pyrometers represents one of the most significant advantages of the technique. The RTC measures an averaged temperature over the circle that it traces out. For increased accuracy, the rotating speed is increased, but the area over which the RTC records and averages remains the same, which means that there is no tradeoff between accuracy and spatial resolution in the RTC. This is not the case with the suction pyrometer: the accuracy of the measurement is dependent on the amount of gas aspired into the suction pyrometer and the spatial resolution of a suction pyrometer reduces as the velocity at which gas is aspirated increased, Fig 5.1. Shows the non-isokinetic sampling of gas by a suction pyrometer. In any system of practical interest, the gas will have some velocity given by V_{gas}. The suction pyrometer accelerates that gas to the desired aspiration velocity, given by V_{sp}.

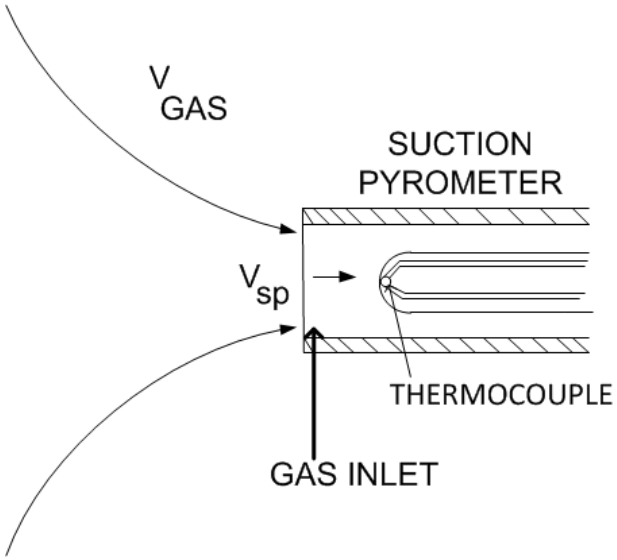

Fig. 5.1. Schematic illustrating non-isokinetic sampling of suction pyrometer.

Based on a simple continuity argument, therefore, the effective "area" of gas sampled by the suction pyrometer is therefore given by:

$$A_{Sampled} = (\frac{V_{sp}}{V_{gas}})A_{SP} \quad (5.1)$$

Where V_{SP} is the aspiration velocity of the suction pyrometer, V_{gas} is the velocity of the gas being sampled, $A_{sampled}$ is the region of gas sampled by the suction pyrometer and A_{SP} is the area of the suction pyrometer's inlet. The spatial resolution of the suction pyrometer, therefore, is system dependent in that it is heavily dependent on the velocity of the gas being sampled. However, since aspiration velocities are typically an order of magnitude greater than the velocities of the gases being sampled, the sacrifice in spatial resolution is extremely significant.

5.3 Averaging over Space and Time

Fig. 5.2a shows the circle traced out by an RTC with a rotational radius '*r*', rotating at a speed *ω* in a temperature field. The temperature field is shown in Fig. 5.2b. If the RTC were allowed to reach steady-state at each point θ along the circle, then it would measure a temperature distribution $T_{b,\theta}$, based on the varying temperature field as θ varies from 0 to 2π. This is represented by the solid curve $T_b(\theta,\omega_0)$ in Fig. 5.2b. If ω was any positive nonzero value, then the RTC would not be able to reach steady-state at any point along the circle, resulting in a flattening of the curve $T_b(\theta,\omega_0)$, and a lag, the magnitude of both of which are dictated by the time constant of the RTC, τ_b. As ω is increased relative to τ_b, $T_{b,\theta}$, will further flatten out, as shown by curves $T_b(\theta,\omega_1)$ and $T_b(\theta,\omega_2)$ in Fig. 5.2b.

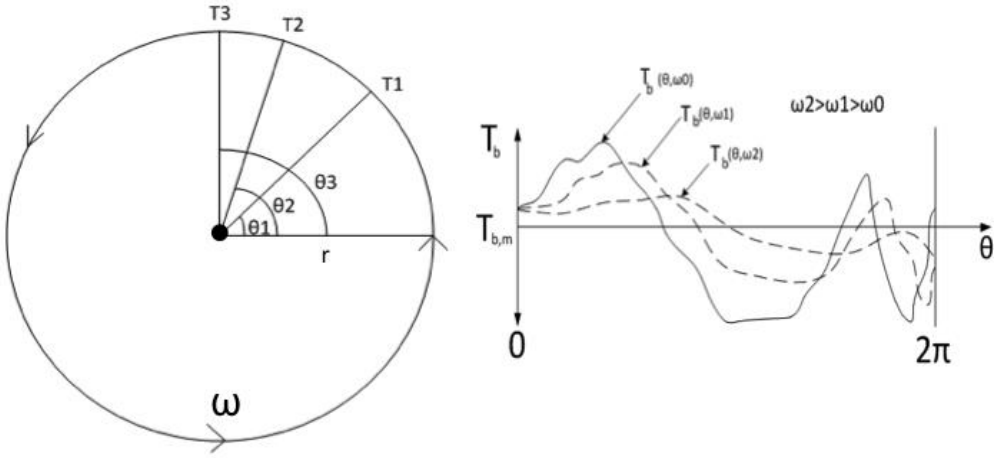

Fig. 5.2. Averaging over circle traced out by RTC. (a) RTC rotating with a radius *r* and a rotational speed ω in a temperature field, (b) shows the temperature measured by the RTC in the temperature field at different rotational speeds.

5

Table 5.2 shows the relative magnitude of the RTC time constant and the time taken to traverse the circle at two rotational speeds of interest, for a range of bead diameters. It is apparent that at both rotational speeds, 5,000 rpm and 10,000 rpm, τ_b is much longer than the time taken to traverse the circle once, and is therefore insensitive to changes in the temperature over the circle. The RTC therefore measures a single mean temperature while rotating around a point, $T_{b,m}$ as it traverses the circle, at sufficiently high rotational speeds.

Table 5.2. Calculated Relative magnitude of RTC time constant relative to rotational speed

Bead Diameter (mm)	Time Constant, τ_b at 5,000 rpm (seconds)	Number of circles swept in one time constant at 5,000 rpm	Time constant, τ_b, at 10,000 rpm (seconds)	Number of circles swept in one time constant at 10,000 rpm
0.30	0.46	38	0.36	60
0.20	0.24	20	0.19	32
0.13	0.11	9	0.09	15

If the temperature field that the RTC is spinning in experiences a change on a time-scale that is significantly longer than τ_b, then it can completely capture this change, as a normal non-rotational thermocouple would. Similarly, if the temperature field changes a time-scale that is significantly shorter than τ_b, then the RTC would not be able to capture these changes. If the change were on the order of the time-constant of the thermocouple, then the rotation would average the measurement in both space and time. These ideas are summarized in table in Table 5.3.

Table 5.3. Averaging in Time

Condition	T_b
$\tau_b << t_{change}$	Captures change in temperature field
$\tau_b >> t_{change}$	Cannot capture change in temperature field
$\tau_b \approx t_{change}$	Average over space and time

5.4 Deconvolution

Since the RTC measures a constant, averaged temperature $T_{b,m}$, it is possible to construct a methodology by which its measurements in a temperature field can be deconvolved to yield spatial resolution approaching that of the diameter of the thermocouple wire. Let $f(x_1,y_1)$ be the temperature at a point (x_1,y_1) on the two-dimensional plane under investigation, $h(x_1,y_1)$ be the impulse function of the RTC measurement system, and $g(x_1,y_1)$ be the measurement obtained from a thermocouple when it rotates along a circle whose center is (x_1,y_1). These are illustrated in Fig.5.3. From convolution theory we know,

$$g = f * h, \tag{5.2}$$

where $*$ indicates the convolution operation. To simplify the calculation, we discretize f, g, and h into block grids. By doing so, the coordinates (x, y) are no longer made of real numbers indicating the exact location. Instead, they are made of integers indicating the indices of a certain block in the grid. Also, the integral involved in the RTC measurement system is simplified to a sum, and thus the impulse function h is significantly simplified to a two-dimensional grid with blocks being $\frac{1}{N}$ if crossed by the circumference and 0 otherwise, where N

is the total number of blocks crossed by the circumference. Such a discretized impulse function is equivalent to a filter or mask in digital image processing, and corresponding deconvolution algorithms can be found in [47].

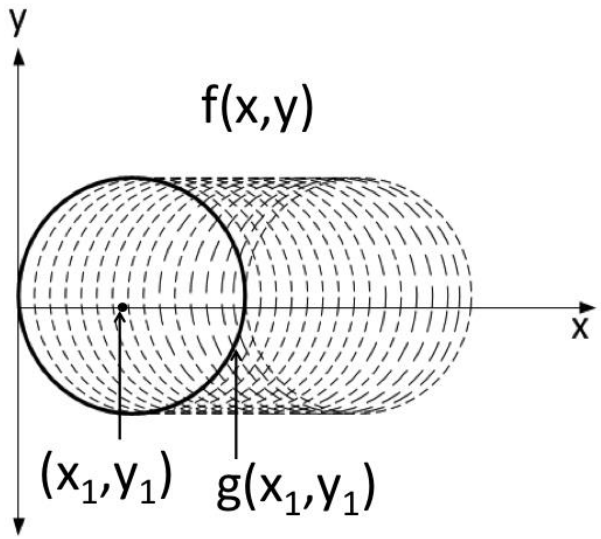

Fig. 5.3. Schematic of deconvolution operation.

Fig. 5.4. shows the results of the deconvolution simulation. In Fig. 5.4a, a temperature distribution is assumed between 20˚C and 1000˚C over a 2-Dimensional plane that is 100mm × 100mm. The plane is then discretized with each grid square measuring 1mm × 1mm. An RTC with rotational radius 10mm is then swept across the plane in both the x- and y- directions, with each new RTC measurement centered at the next grid point. This "measured" distribution, *g(x,y)* is shown in Fig. 5.4b. The deconvolution operation is then applied to the measured distribution in Fig 5.4b. to yield a deconvolved distribution, shown in Fig. 5.4c.

The deconvolved distribution is in excellent agreement with the original distribution. The RMS error of the deconvolved distribution is 0.37°C, while the RMS error of the measured distribution is 24°C. The distribution of this error for the deconvolved distribution is shown in Fig. 5.4d.

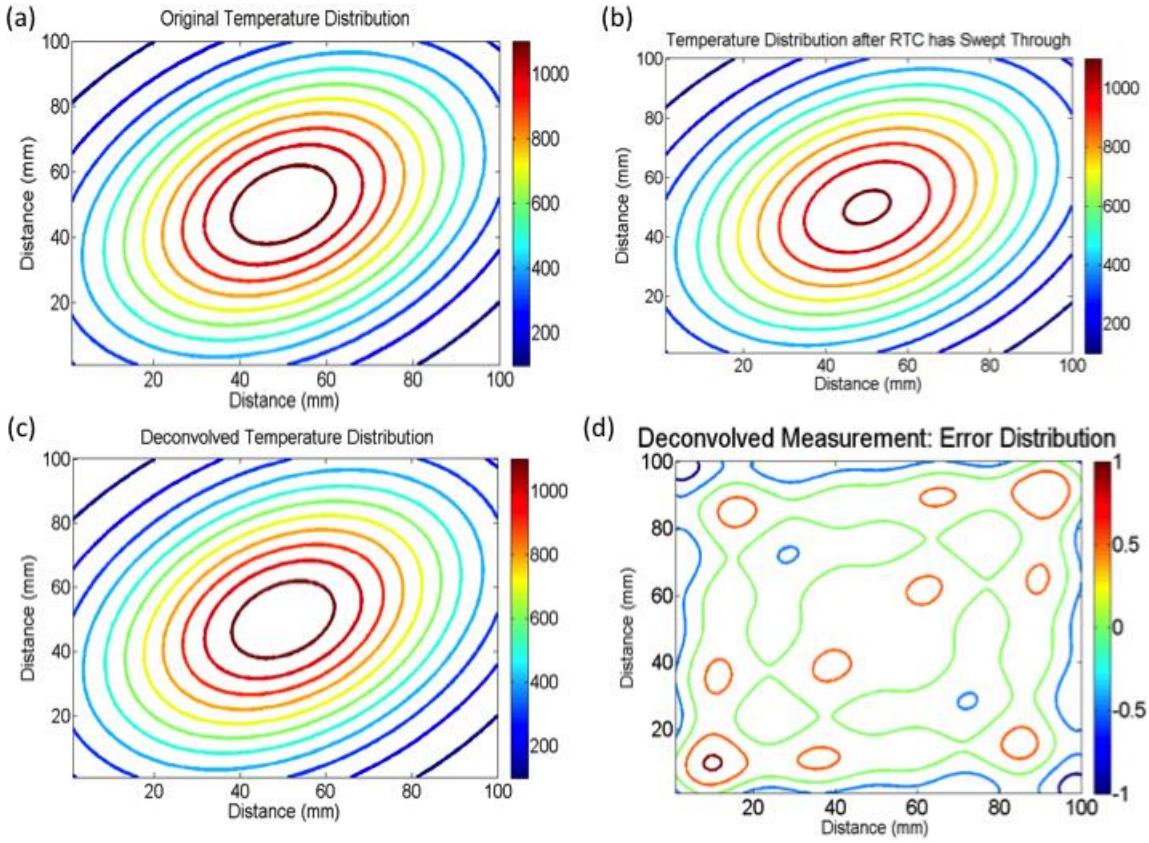

Fig 5.4. Results of deconvolution simulation. (a) Original temperature distribution, (b) measured temperature distribution after RTC as swept through, (c) Deconvolved temperature distribution, (d) distribution of error after deconvolution operation.

Chapter 6

Future Work

It has been shown in this work that high-speed rotation can significantly improve the accuracy of thermocouple measurements in radiating flame environments. However, this work represents a preliminary proof-of-concept, and there remain challenges in the design and optimization of a RTC that will be feasible in larger systems. For example, in order to be accessible to measurement ports in many burners, the RTC needs to be significantly longer, which entails nontrivial design challenges.

The RTC essentially represents the ability to control the local convective heat transfer coefficient over an extremely small area, which opens up a host of interesting research directions. Based on measurements, a complete 3-D mapping of local gas properties, such as the Prandtl number and the viscosity could be possible. The RTC also opens up alternative approaches to measuring temperature. The time-constant of a thermocouple is strongly dependent on the local convective heat-transfer coefficient, so it should be possible to accurately measure the time constant of a thermocouple as a function of rotational speed, and extrapolate to find a gas temperature in this way. The technique could also be used to accurately calibrate optical temperature measurement techniques, through the imaging and measurement of the RTC's irradiance at different rotational speeds.

Finally, the deconvolution scheme introduced here represents a preliminary step, with the ultimate goal of having spatial resolution on the order of one thermocouple diameter.

Chapter 7

Conclusion

In this work, the challenges associated with accurate temperature measurement using thermocouples in large, radiating flame environments is presented, along with the limitations of techniques currently in use. A framework for a Rotational Thermocouple (RTC) is presented that seeks to alleviate many of the inaccuracies that currently limit temperature measurement. An experimental system has been constructed that tests the ability of a RTC to make accurate flame-temperature measurements. The results show a significant reduction in the required value of the correction, while the semiempirical curve-fit yields a temperature value that is within 15 K of the calculated value using radiative correction. A deconvolution methodology has also been introduced, which could improve the spatial resolution to the level of a point measurement of a thermocouple. These results are summarized in Table 7.1.

Table 7.1. Summary of Results

	Fine-Wire Thermocouple	Suction Pyrometer	High-Speed Rotational Thermocouple (RTC)
Accuracy	High; Fine-wire minimizes radiation losses, though they may still be present.	Moderate; Inaccuracies of hundreds of degrees kelvin can persist even with high-speed aspiration.	Very high; Can fit data to theory to get true gas temperature.
Spatial Resolution	Very high high; limit of resolution is surface area of fine-wire thermocouple, on the order of $10^{-9}m^2$.	Poor; Can be on the order of $1m^2$; significant tradeoff between increased accuracy and precision.	High; Can deconvolve measurements to get spatial resolution approaching that of bare-bead thermocouple. No tradeoff between increased accuracy and precision.
Temporal Resolution	Extremely high owing to small mass of thermocouple; Time constant on the order of 50-100ms.	Very poor due to presence of shields; Time constant on the order multiple minutes.	High; Time constant is higher than that of a fine wire thermocouple, but RTC also averages over space and time, so temporal resolution is not as high as that of fine-wire thermocouple.
Mechanical Integrity	Very poor; Extremely fragile.	Robust due to presence of shields.	Moderate to high; Thermocouple wire diameter is larger than that of a fine-wire thermocouple, and shielded, but not completely enclosed like suction pyrometer.
Time to Take Measurement	Very low.	Very high, due to presence of shield.	Very low
Maintenance	Very High; Fragility causes frequent breakage,	Very High due to clogging with particles.	Anticipated to be low;

Appendix

Nomenclature

A	Area (m^2)
D	Diameter of bead (m)
h	Convective Heat Transfer Coefficient (W/m^2-K)
RTC	Rotating thermocouple
L	Length (m)
$\dot{Q}$	Heat Flux (W)
r	Radius (m)
T	Temperature (K)
V	Velocity (m/s)
ω	Rotational speed ($revolutions/min$)
σ	Stefan-Boltzmann Constant $(5.67051 \times 10^{-8} \frac{W}{m^2K^4})$
ε	Emissivity
k	Thermal Conductivity $(\frac{W}{m-K})$
μ	Dynamic Viscosity $(\frac{kg}{m-s})$
ϱ	Density
t	Time
τ	Time constant

Subscripts

b	Bead (thermocouple bead)
cr	Cross Section
D	Diameter
g	Gas
s	Surface
w	Wall

Dimensionless Numbers

Bi	Biot Number,
Nu	Nusselt Number,
Pr	Prandtl Number,
Re	Reynolds Number

References

[1] E.I.A., *Global Energy Outlook,* 2011, Energy Information Administration, 2011

[2] Law, C.K., *Combustion Physics*, Cambridge University Press, 2006.

[3] Bradley, D., Matthews, KJ., *Journal of Mechanical Engineering Science*, **10.4**(1968)

[4] Heitor, M.V and Moreira, A.L.N, *Prog. Energy Combustion Science*, **19**(1993) 259-278

[5] Bahlawane, N., Struckmeier, T., Kasper, T.S., Oswald, P., *Review of Scientific Instruments*, **78,** 018905 (2007).

[6] Katsuki, M., Mizutani, Y., Matsumoto, Y., *Combustion and Flame* **67** 27-36 (1987)

[7] Bradley, D., Lau, A.K.C., Missaghi, M., *Combustion Science and Technology*, **64**119-134 (1989)

[8] Tagawa, M., Ohta, Y., *Combustion and Flame*, **109**:549-560 (1997)

[9] Brohez, S, Delvosalle. C, Marlair. G*, Fire Safety Journal*, **39** (2004) 399-411

[10] Hung, P.C., Irwin, G., Kee, R., Mcloone, S., *Review of Scientific Instruments* **76**, 024902 (2005)

[11] Blevins. L, Pitts. William, M., *Fire Safety Journal*, **33.4**,1999

[12] Pitts, W.M., Braun, E., Peacock, R.D., Mitler, H.E., Johnsson, E.L., Reneke, P.A., and Blevins, L.G., "Temperature Uncertainties for Bare-Bead and Apsirated Thermocouple Measurements in Fire Environments", *Thermal measurements: The Foundation of Fire Standards, ASTM, STP 1427* L.A Gritzo and N.J Alvares, Eds., ASTM International, West Conshohocken, PA, 2002.

[13] Kim, S.C., Hamins, A., *Journal of Fire Sciences*, **26**(2008) 509-528

[14] Newman, Jeffrey. S., Croce, Paul. A., *Journal of Fire and Flammability*, **10** (1979) 326-336

[15] Z'Graggen, A., Friess, H., Steinfeld, A., *Measurement Science and Technology*, **18**(2007) 3329-3334

[16] Churchill, S.W., Bernstein, M., *Journal of Heat Transfer- Transactions of the ASME*, Vol. 99, Issue 2, 300-306, 1977

[17] Incropera, F.P., DeWitt, D.P., Bergman, T.L., Lavine, A.S., *Fundamentals of Heat and Mass Transfer*, 6th Ed., Wiley and Sons, 2007.

[18] Migliorini, Fr., De Iuliis, S., Cignoli, F., Zizak, G., *Combustion and Flame*, **153** (2008) 284-393.

[19] Gregor, M.A., Driezler, A., *Measurement Science and Technology*, **20** (2009) 065402 (FF BURNER)

[20] Sutton, G., Levick, A., Edwards, G., Greenhalgh, D., *Combustion and Flame* **147** (2006) 39-48

[21] Mammoser, J.H., Jimenez, A., "Comparison of Temperature Measurements in Fire Test Furnaces Using Aspirated Thermocouples", *Proceedings of HT 2005,* ASME Summer Heat Transfer Conference, San Francisco, CA., 2005.

[22] Kent, J.H., Bilger, R.W., *Fourteenth Symposium (International) on Combustion*, p. 615, The Combustion Institute, Pittsburgh PA, 1973

[23]Sato. A., Hashiba, K., Hasatani, M.., Sugaiyama, S., Kimura, J., *Combustion and Flame*., **24** 35, (1975)

[24]Hayhurst, A.N., Kittleson, D.B., *Combustion and Flame*, **28,** 301, (1977)

[25]Vishkanta, R., Menguc, M.P., 1987, *Progress in Energy and Combustion Science,* **13**, 97-160, 1987.

[26]Attaya, A.M., Whitelaw, J.H., *ASME Pap 81-WA1HT-6* (1981).

[27] Moneib, H.A., Experimental Study of the Fluctuating Temperature in Inert and Reacting Turbulent Jets, PhD. Thesis, University of London, 1980.

[28]Bradley, D., Entwistle A.G., *Journal of Applied Physics*., **12**, 708, 1961

[29] Kent, J.H., Bilger, R.W., Charles Kolling Research Laboratory, *Technical Note F-34* (1972)

[30]Sbaibi, A., Parenthoen, P., Lecordier, J.C., *Journal of Applied Physics E. Scientific Instruments*, **22**, 24, 1989.

[31]Parenthoen, P., Petit C., Lecordier, J.C., *Journal of Fluid Mechanics*., **124**, (457) (1982)

[32] Petit, C., Gajan P., Lecordier, J.C., Parenthoen., *Journal of Physics E. Scientific Instruments,* **15**, 760, 1982.

[33]Parenthoen, P., Lecordier, J.C., Petit C., and Gajan, P., *8th Australasian Fluid Mechanics Conference*, pp 6B.1-6B.4, University of Newcastle (1981).

[34] Shaw, D.W., Essenhigh, R.H., *Combustion and Flame*., **86**:333-346 (1991).

[35]Guo, Y., Chan C., Lau K., *Fuel*, **82**, 893-907, 2003.

[36] Holderness, F.H., Tilston, J.R., MacFarlane, J.J., Electrical Compensation for Radiation Loss in Thermocouples National Gas Turbine Establishment, *Note No. NT 758* (1969).

[37] Khalil, M.B., Whitelaw, J.H., *Sixteenth Symposium (International) on Combustion*, p. 569, The Combustion Institute, Pittsburgh, PA, 1977.

[38]Odidi, A.DD., Imperial College of Science and Technology, Mechanical Engineering Department, University of London, (1974)

[39]Bilger, R.W., *Progress in Astronautics and Aeronautics,* B.T Zinn (Ed.) **53**, 44 (1977).

[40] Schnonung, S.M., Hanson, R.K., *Combustion Science and Technology*, **24** 227, (1981).

[41] Toral, H., Whitelaw J.H., *Combustion and Flame*, **45**, 251 (1982)

[42]Heitor, M.V., Taylor, A.M.K.P., Whitelaw, J.H., *Combustion Science and Technology*, **6**, 297 (1988).

[43] Whitaker S., Forced convection heat transfer correlations for flow in pipes past flat plates, single cylinders, single spheres, and for flow in packed beds and tube bundles. AIChE Journal, **18**, 1972, 361-371.

[44]Omega Temperature Handbook, Omega Engineering Incorporated, 1996

[45] Luckerath, R., Woyde, M., Meier W., Stricker, W., Schnell, U., Magel. H., Gorres. J., Hartmut, S., Maier H., *Applied Optics*, **34**, 3303-12, 1995.

[46]Childs. P.R.N., Greenwood, J.R., Long, C.A., *Review of Scientific Instruments*, **71**, 2959-79, 2000.

[47] Gonzalez, R.C., Woods, R.E., Eddins, S.L., *Digital Image Processing Using MATLAB*, (2003) 108–140.

Vita

Siddharth Krishnan

Degrees

M.S, Mechanical Engineering, Washington University in St. Louis, May 2014
B.S. Mechanical Engineering, Washington University in St. Louis, May 2013

Professional Societies

American Society of Mechanical Engineers
Combustion Institute

Temperature Measurement in Flames, Krishnan, M.S 2014